Advanced Ultrathin Spray Coating Process Technology for Heterogeneous Integration Applications

Johanna Rimböck
EV Group E.Thallner GmbH
St. Florian am Inn, Austria
j.rimboeck@evgroup

Stefan Ertl
EV Group E.Thallner GmbH
St. Florian am Inn, Austria

Prasanna Ramaswamy
X-Celeprint Limited
Cork, Ireland

Alex Farrell
X-Celeprint Limited
Cork, Ireland

Ali Uzun
Photonics Research Group, INTEC
Ghent University - imec,
Ghent, Belgium

Mariana Pires
EV Group E.Thallner GmbH
St. Florian am Inn, Austria

Brian Corbett
Tyndall National Institute
Cork, Ireland

Ruggero Loi
X-Celeprint Limited
Cork, Ireland

Ksenija Varga
EV Group E.Thallner GmbH
St. Florian am Inn, Austria

Peter Ossieur
IDLab, INTEC,
Ghent University - imec
Ghent, Belgium

***Abstract* — In this work the spray coating deposition of thin and ultrathin homogeneous layers of Divinylsiloxane-bis-benzocyclobutene (DVS-BCB or BCB) is presented. Film thicknesses from 200 nm down to 5 nm are achieved. The layer thickness is assessed using Variable Angle Spectroscopy Ellipsometry (VASE), which allows for nondestructive high precision thickness measurement. Multiple positions mapping provides information about thickness distribution across the substrate. This spray coating process study reveals that the layer deposition for thicker films (> 75 nm) is mainly driven by hardware parameters. For thinner layers, additional material solution adjustment (dilution) is necessary. For each studied layer thickness (200 nm, 35 nm and 5 nm), batches of 25 wafers are prepared aiming to study the wafer-to-wafer process stability necessary for successful industrial application. Finally, the thin and ultrathin BCB layers are used for different bonding technologies, i.e. die-to-wafer permanent adhesive bonding as well as micro transfer printing (µTP). Multiple electronic integrated circuits (EICs) and quantum dot lasers (QDLs) devices are heterogeneously integrated to Si/SiO_2/BCB wafers using the layers with thicknesses of 35 nm and 5 nm. For all devices a 100 % process yield is obtained.**

Keywords* — *ultrathin layer, spray coating, micro transfer printing µTP, ellipsometry, adhesive bonding, die-to-wafer bonding, silicon photonics, electronic integrated circuits EICs, quantum dot lasers QDL

I. Introduction

Wafer-to-wafer (W2W) and die-to-wafer (D2W) processes are becoming more important nowadays due to their wide field of applications. However, such processes are extremely demanding and challenging due to the strict requirements in terms of surface quality, e.g. (i) extremely low roughness, (ii) chemical affinity between bonded surfaces, (iii) very high flatness over the entire bonding area. Such requirements are easy to meet for blank SEMI standard Si wafers but often difficult to meet for more advanced and fully processed substrates. In order to overcome the surface quality challenge, heterogeneous integration technology was developed and becomes more and more important in the semiconductor industry. The use of an intermediate layer for bonding can be a good solution to overcome the demanding requirements on the substrate surface quality [1,2,3]. An intermediate layer can be used to reduce the existing surface roughness and to overcome small surface irregularities. The use of interfacial adhesive layers is important also as it facilitates the bonding of different materials which cannot be bonded using a direct bonding process. In the recent years, the heterogenous integration processes started to attract the industry attention. In such concept, due to the lack of standards in terms of language, heterogenous integration is sometimes referred to as consisting of integration of non-silicon materials in silicon industry (e.g. compound semiconductors integrated in silicon manufacturing technology) but also as the integration of separately manufactured components into a higher level assembly (System-in-Package, SiP) that, in the aggregate, provides enhanced functionality and improved operating characteristics [1,2,4]. The work described here is important for both integration schemes as it provides a method allowing for overcoming complex and expensive surface preparation methods by simply employing a polymer layer.

The wafer bonding processes currently in use are typically categorized into two classes: (i) direct bonding and (ii) bonding using intermediate layers. Besides the inherent benefits for some applications, the direct bonding technique is the most demanding in terms of surface quality requirements. The use of intermediate bonding layers is typically loosening the requirements for surface quality, and this can be a benefit for some categories of applications. Among the materials suitable as

The presented work was supported by European Union's Horizon 2020 innovation programme (Caladan, no.825453).

bonding layers, organic materials can be employed due to their physical and chemical properties which can be further tuned by chemical engineering [5,6,7,8]. One of the most common materials used as an intermediate adhesive layer for bonding is Divinylsiloxane-bis-benzocyclobutene (DVS-BCB or BCB) due to its (i) good thermal stability, (ii) low dielectric constant, (iii) extremely low moisture absorbance, (iv) excellent adhesive characteristics, and (v) relatively easy handling [8,9,10].

The choice of the proper adhesive bonding process consists not only of choosing the appropriate material, but also the proper deposition process to ensure the bonding requirements are met. The method should provide a stable and well controlled environment allowing for the deposition of layers with thicknesses from the micrometer down to the nanometer scale. For the bonding process, the layer thickness has to be correlated with the substrate properties (i.e. roughness, bow, topography). The use of highly bowed/warped and/or patterned wafers would demand for intermediate bonding layers with thicknesses in the micrometer range. For heterogenous integration applications this demand can be easily downscaled to the nanometer range due to the higher quality of the substrates employed compared to other applications. In addition, an appropriate deposition technique should offer the possibility of coating the material onto non-round shaped substrates as well as over nano-/micro-structured surfaces. Ideally, it should allow for high throughput and low material consumption, thus increasing the cost efficiency. Although being one of the well-established techniques which can provide high quality results in terms of layer homogeneity and thickness control, spin coating is fast reaching its limits when non-round shaped and/or patterned samples are employed. Other methods, e.g. blade coating, electrochemical deposition/polymerization are subject to numerous limitations which make them hard to be considered as candidates for industrial applications in bonding technology [11,12,13]. By comparison, spray coating is a good candidate which can fulfill all above mentioned requirements. Although it is used typically to prepare layers with thicknesses in the micrometer range, it was previously shown that a 125 nm layer could be successfully prepared and used as bonding intermediate layer [14]. Also, high process stability and repeatability was already proven [14]. Additionally, the spray coating operation principle allows for performing coating with extremely low amount of material (down to microliters) with almost no material loss, which is outstanding when considering the material costs. Although thin layers in the nanometer scale were prepared and their applicability was proven, further thickness downsizing would be of great importance for reduced integration biases and improved thermal sink [1]. Layers with thicknesses of only few nanometers could be beneficial as they combine the advantages of adhesive bonding (e.g. less strict surface requirements) with the properties of direct bonded interfaces, e.g. in terms of thermal properties. For example, a very thin layer of BCB shows a thermal conductivity of the bonded interface similar to direct bonding [15]. On the other hand, for III-V lasers used with silicon photonics applications, a short distance between laser and the SOI (Silicon-on-Insulator) waveguide in an evanescent light coupling layout minimizes light losses and thus significantly increases the efficiency of the bonded devices [1]. A thin adhesive layer can (i) reduce stress in the bonded interface, and (ii) help compensate for small flatness issues or surface roughness of chips [16]. Moreover, a very thin layer can reduce the risk of misalignment of bonded coupons during the curing step due to less reflow as well as less shrinkage of the material [17].

The goal of this work was to develop an advanced spray coating process for layer thickness down to 5 nm and show the applicability of such thin layers for heterogenous integration applications. The first step towards this was the preparation of layers with various thicknesses to prove the level of process control as well as its high reproducibility and repeatability. All wafers were characterized using variable angle spectroscopic ellipsometry (VASE), which is a non-destructive metrology method with mapping capabilities and very high precision (< 1 nm). As this method demands mathematical modelling to provide the requested layer parameters (thickness, optical roughness), for each target layer thickness 5 wafers were additionally analyzed using an atomic force microscope to confirm the developed VASE model correctness. Finally, a thin layer application in the heterogeneous integration for integrated photonics will be presented. Electronic circuit, as well as GaAs based lasers were integrated using the micro transfer printing (µTP) technology on Si wafers which were spray coated with BCB layers thinner than 40 nm. The µTP is a relatively new technology, which enables new solutions for the creation of co-packaged optics with high thermal performance.

II. Materials and Methods

A. Spray Coating Deposition and Layer Characterization

All samples were prepared using EVG Omnispray® Technology. The system is using an ultrasonic spray nozzle allowing for a very high atomization and droplet size stability and leading to homogeneous layer deposition with high throughput [18]. For all experiments, BCB from Dow Chemicals (Cyclotene 3022-46) was used. For specific tests BCB was diluted using Mesitylene (Dow Chemicals, Rinse T1100) to adjust the viscosity to a level suitable for spray coating. The material preparation/dilution was shown to be crucial to define the target thickness of the adhesive layer. Dilutions were defined to cover a very broad range of thicknesses, from 5 nm to 200 nm. The details about the hardware and process parameters were reported in previous works [14,19].

The BCB layers were spray coated on top of single side polished Si wafers (200 mm diameter with <100> crystal orientation), native oxide was not removed before coating. After deposition, all samples were soft baked using a hotplate at 90 °C for 60 seconds in 500 µm proximity. The soft bake process should ensure full and homogeneous sample drying.

All prepared samples were analyzed using variable angle spectroscopic ellipsometry (VASE). This technique allows fast, non-destructive, and very precise (down to 1 Å) measurements. For these tests, a semi-automated Woollam M-2000 ellipsometer was used. 49 points were measured on each sample using cartesian, equidistant position distribution. A measurement spot size of roughly 3 x 5 mm^2 was used for a wide spectral range measurement (with wavelengths from 190 nm to 1687 nm). Three angles of incidence were applied (AOI 60°, 65° and 70°) to achieve the highest precision. The angle choice

is related to the Brewster Angles of BCB and substrate materials, allowing the highest measurement sensitivity. The polarization change was detected in form of Ψ and Δ functions and analyzed using the CompleteEASE software [20]. For all analysis, a multilayer model was designed to precisely determine the layer thickness. For the simplicity of the analysis process, Cauchy functions were used to describe the BCB layer, while existing libraries of the crystalline silicon and the native oxide were used to describe the substrate [21]. In this study, two parameters were of special interest – (i) optical thickness and (ii) optical roughness. To confirm the VASE modelling, an atomic force microscopy (AFM, PARK system NX20) measurement was additionally performed to determine the BCB layer thickness and the related surface roughness.

B. Die-to-Wafer Bonding

The applicability of the thin and ultrathin layers of BCB was first tested using a permanent Die-to-Wafer bonding process. 7 x 9 mm² Si/SiO_2 dies were bonded on several 200 mm Si/native SiO_2 wafers coated with various BCB layer thicknesses using an EVG®520IS semi-automated bonding equipment. The obtained bond quality was inspected using a Scanning Acoustic Microscope working in C-mode (C-SAM, SAM450 – PVA Tepla Analytical Systems) with a 110 MHz transducer and a resolution of 50 µm/pixel.

C. Micro Transfer Printing

Non-functional electronic integrated circuits (EICs) as well as quantum dot lasers (QDL) transfer printable devices were used to test the heterogenous integration by using micro transfer printing (µTP). The EIC devices were fabricated with a 0.13 µm SiGe BiCMOS technology as shown in previous work and have a foot-print size of 230 x 330 µm² and a total thickness of about 15 µm given by a 13 µm thick back end of line layer stack seating on top of 1.5 µm thick front end of line silicon layer positioned on top of a 1 µm thick buried oxide (box) [22,23]. The box is on a Si substrate with <100> crystal orientation which works as a sacrificial layer for the release of the device from the original wafer. The release technology is based on a process using a TMAH:DI (1:4) etching solution stirred at 70 °C for 2 h and at 40 °C for another 6-8 h in order to achieve the complete undercut of the coupons.

The QDLs used in this manuscript have a ridge waveguide and etched facet with contact pads for electrical connection at the top and were fabricated using standard III-V processing technology similar to prior work [24,25]: The fabrication of the coupons started with the singulation of the rectangular mesas by using a PECVD SiN dielectric hard mask. The inductively coupled plasma etching was performed with BCl_3-Cl_2-N_2-Ar chemistry. The etching process was stopped just before reaching the sacrificial layer with 40 nm SiN remaining on the coupon surface. Next, a SiO_2 layer was deposited by PECVD to encapsulate the top and the sidewalls of the coupons. In a final step a dry-etch process was performed using the same chemistry, allowing the remaining GaAs layer and AlGaAs sacrificial layer to be etched down to the GaAs substrate with a 400 nm over etch. A resist-based anchor system held the coupon to the substrate through engineered tether structures during the undercut. The resulting devices gained from this process were 3.94 µm thick including the remaining 40 nm SiN and 200 nm SiO_2 layers. The lasers were fabricated in form of large aspect ratio coupons with 65 µm width and lengths: (i) 1500 µm, (ii) 1800 µm and (iii) 2400 µm length, respectively. The laser coupons were released from the carrier wafer using a diluted HCl:DI water (1:1) etching solution at room temperature. Different stamps with post size matching the top of the coupon area were used to pick-up and transfer print the different devices. A single post stamp of 200 x 300 µm² size was used for the µTP of the EICs. For the µTP of the QDLs, 60 x 1500 µm², 60 x 1800 µm² and 60 x 2400 µm² posts were used. Standard X-Celeprint technology was used to fabricate the stamps made by Polydimethylsiloxane (PDMS) material [23,24,26].

The µTP tool model used in the print trials was an MTP-200 which uses image recognition software to automatically align the coupon to the receiving substrate. EICs were picked-up with an acceleration of 0.9 g and printed on the landing spots with a 30 µm overdrive; the same values were used for the transfer printing parameters when integrating the QDLs by µTP.

III. Results and Discussion

A. Spray coating

a) Ultrathin Layer Deposition

At first, the applicability of the spray coating technology for ultrathin layer preparation was studied. Several sets of samples with various layer thicknesses were prepared. BCB was the material of choice due to its well-known use in heterogeneous integration applications [3,8,16]. As BCB physical and chemical properties are well known, it was straight forward to exclude from this work the material evaluation and focus on the study and optimization of the spray coating process to obtain the targeted results. All layers were deposited on Si wafers. In the previous reports it was shown that layers with thicknesses between 25 nm and 200 nm could be prepared using the spray coating technology [14,19]. However, coating of thinner layers was at that time too challenging as the previous works focused only on the thickness dependance on the process parameters and kept the BCB material composition constant, so the influence of the material composition was at the time not studied. In order to study the thickness dependence of various BCB material compositions, the material was diluted with Mesitylene in different ratios. The process parameters and material composition leading to a 200 nm layer thickness were chosen as a reference, according to previous reports [14,19]. Samples with layer thickness varying between 5 nm and 200 nm were prepared with a strong focus on thicknesses below 50 nm. All samples were measured using the VASE technique. Ellipsometry allows for non-destructive mapping of the layer thickness and the calculation of the optical roughness over the entire wafer surface. The layers

were further locally analyzed using an Atomic Force Microscope (AFM) to cross-check the mathematical models used in the process of VASE data analysis. For AFM thickness measurements, layers were scratched in 5 different positions and the height difference between the top of the layer and the bottom of the scratch was used to determine the total layer thickness. In order to keep statistical relevance and reasonable measurement time throughput, AFM measurements were performed on every fifth wafer out of the lot of 25 wafers. The measured thickness values for ultrathin layers with target thickness of 5 nm, 8 nm, 17 nm and 35 nm were compared with the 200 nm thick reference BCB layer with respect to the targeted thickness values. The average VASE and AFM results are summarized in Table 1.

TABLE I. THICKNESS VALUES DETERMINED BY VASE AND AFM MEASUREMENTS FOR DIFFERENT TARGET THICKNESSES.

Spray Coated Layer Thickness						
		Target Layer Thickness				
		5 nm	***8 nm***	***17 nm***	***35 nm***	***200 nm***
VASE	***Average Optical Thickness***	4.3 nm	8.0 nm	18.1 nm	35.3 nm	189.6 nm
	Minimum Optical Thickness	3.8 nm	7.1 nm	16.2 nm	31.1 nm	157.6 nm
	Maximum Optical Thickness	4.7 nm	8.7 nm	19.7 nm	39.2 nm	214.7 nm
AFM	***Average Thickness***	N/A	9.0 nm	14.0 nm	48.0 nm	173.0 nm

From the data presented in Table 1, it can be concluded that spray coating using the developed process allows for the preparation of layers with thickness accurately matching the target values. A very good understanding of the process parameters relations was achieved in the experiment. It is possible to precisely target any layer with thickness above 4 nm with an error of approx. 1 nm and a wafer-level non-uniformity of ±10%.

When comparing the VASE with the AFM thickness data, it can be noticed that they are in a good correlation. Of course, some differences can be observed, e.g. for 17 nm and 35 nm target thicknesses, but they could be related to the nature of AFM measurement being difficult to ensure that the substrate surface is reached by the tip on the scratched areas, thus ensuring full thickness measurement. A similar description was proposed previously by Llamas, Guzman et al. [27]. Additionally, the differences can be related to the used scanning area. The VASE measurement provides an averaged information from the large light spot (3 x 5 mm²) used while the AFM measures in the micrometer scale (2.5 x 2.5 µm²). It is also known that manual scratching the layer to perform thickness analysis is not the most precise method and does not always lead to controlled and reproducible sample preparation.

In the next step, both VASE and AFM techniques were used to determine the roughness values. Both methods can analyze layer roughness, however they have different approaches, and the obtained results have different physical meanings. From VASE the so called "optical roughness" can be obtained, which describes an optically non-homogeneous layer composed of the surface roughness as well as void inclusions in the layer, thus leading to local variation of the refractive index. On the other hand, the AFM measurement provides surface roughness, analyzed using a combination of mechanical and electrical interactions between the tip of a cantilever and the sample surface. Details about differences can be found elsewhere [14]. The results obtained using both methods are shown in Table 2.

TABLE II. ROUGHNESS VALUES DETERMINED BY VASE AND AFM MEASUREMENTS FOR DIFFERENT TARGET THICKNESSES.

Spray Coated Layer Roughness						
		Target Layer Thickness				
		5 nm	***8 nm***	***17 nm***	***35 nm***	***200 nm***
VASE	***Average Optical Roughness***	2.5 nm	2.1 nm	2.0 nm	1.7 nm	4.6 nm
	Minimum Optical Roughness	1.8 nm	1.6 nm	1.5 nm	1.4 nm	3.4 nm
	Maximum Optical Roughness	3.2 nm	2.6 nm	2.3 nm	2.2 nm	5.6 nm
AFM	***Average Surface RMS Roughness***	0.3 nm	0.3 nm	0.4 nm	0.4 nm	0.4 nm

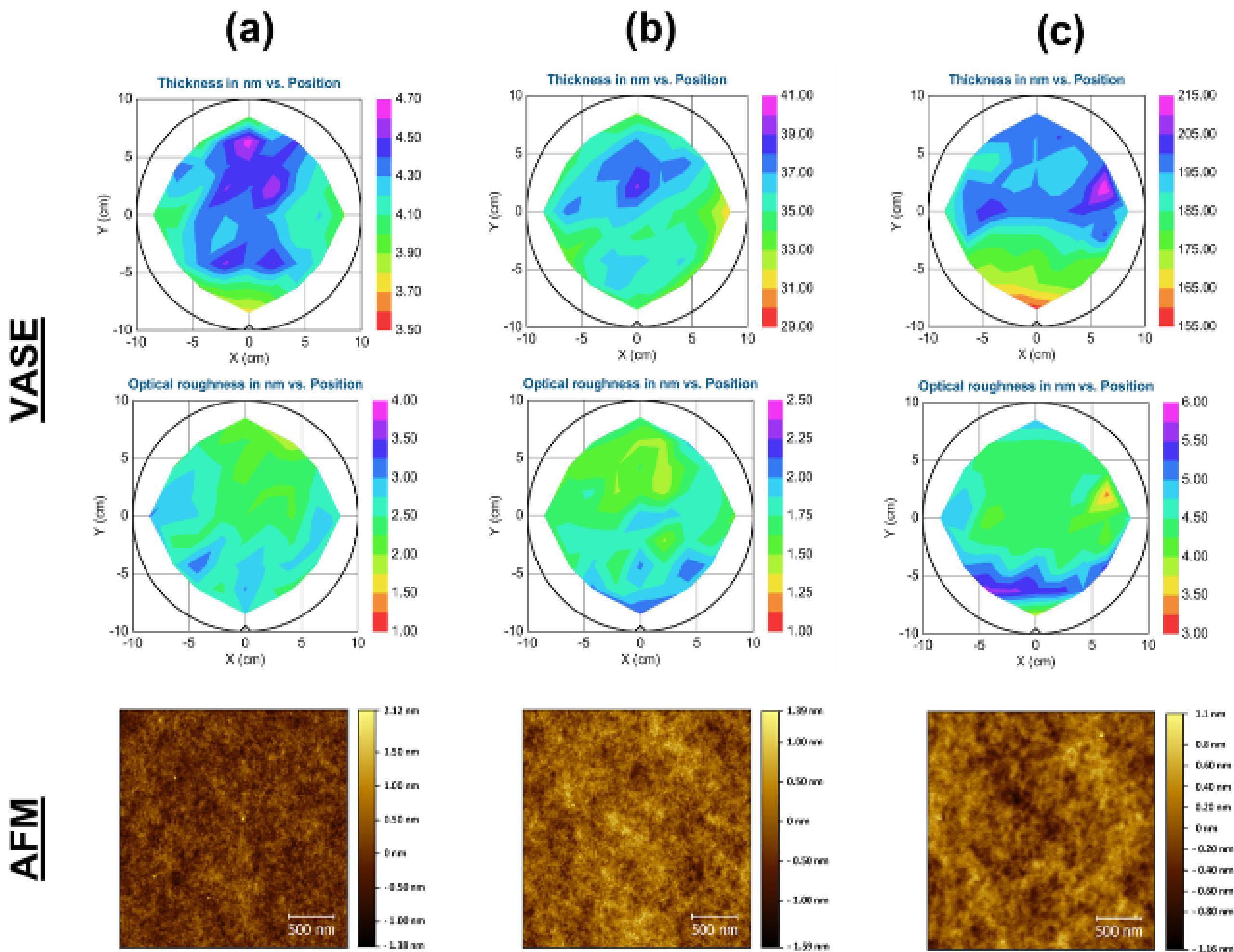

Fig. 1. VASE thickness, VASE optical roughness and AFM surface profile of the height for (a) 5 nm, (b) 35 nm and (c) 200 nm BCB layers on Si wafers.

A large difference between AFM and VASE could be observed but considering the difference between optical and surface roughness definitions, such a high difference is not surprising. It is important that the surface roughness value is equal or, as in the present case, lower than the optical roughness. The optical roughness is calculated using the effective medium approximation (EMA) with 50/50 % ratio of material refractive index to void refractive index. The choice of this ratio is based on the 3D layer description and further described in detail elsewhere [14]. Besides the definition of both physical quantities, there is a difference in the size of the sampling area. Another important difference arises when comparing layers with target thickness equal or lower than 35 nm with the 200 nm reference sample. While AFM results show almost the same surface roughness for all samples, the VASE metrology shows that the optical roughness doubles for the reference sample. For thin layers it seems that the roughness values are constant for both methods. This can be explained by an additional layer present below the surface and consisting of e.g. air voids. Such voids are most likely generated during the drying process during the layer deposition process. For very thick films, surface drying seems to be much faster than mesitylene vapor diffusion through the layer, which could lead to void formation under the already polymerized surface. On the other hand, for ultrathin layers the entire layer volume dries instantly and there is less chance for void formation.

The exemplary measured thickness and optical roughness distribution maps for 5 nm, 35 nm and 200 nm layers target thicknesses together with the according AFM surface scans are shown in Fig. 1.

First, when analyzing the thickness maps determined by VASE, a good layer thickness uniformity over the entire wafer can be observed. Of course, it is well known that spray coating provides samples with significantly lower homogeneity as compared to e.g. spin coating. However, when looking closely, the uniformity value is mainly driven by some few outliers due to the samples not being pre-treated with cleaning or priming steps. The outliers can be caused by various defects i.e. airborne particles, substrate surface defects, dangling bonds, etc. The cleaning and priming steps were not used here as the majority of industrial applications do not allow or allow only for very specific pre-treatment procedures. However, when removing the outliers, a significant improvement of the thickness uniformity is

achieved (e.g. for 35 nm from 11.5 % to 6.9 %). Very high uniformity was achieved for the thinnest film (Fig. 1a) where, after removing outliers, the variation in the layer thickness is in the range of ±4 Å over the 200 mm Si wafer surface. Such quality of

the spray coated layer is an excellent achievement, which fully complies with the bonding process specification [16]. Moreover, the thicker layers presented in Fig. 1b and 1c show a high homogeneity, considering they are obtained by spray coating technology. The observed differences between ultrathin and thin layers again can lead to a conclusion that surface homogeneity can be determined by solvent diffusion and/or evaporation rates.

During the modelling of the VASE measurement, additional analysis on the optical roughness was performed. The optical roughness describes the variation of the dielectric function due to air inclusion, e.g. bumps, holes or air bubbles in the upper region of the adhesive layer. Such region can be considered as a layer that can be mathematically described by using the EMA. Such a definition, based on physical understanding of thin layer formation, is well established in the ellipsometry community, and widely used in data analysis. As it can be noticed in Fig. 1, the obtained values seem to be very similar for all layer thicknesses (around 4 nm for 200 nm reference and 2 nm for all other thicknesses) and almost independent from the chosen target thickness values. However, a 2 nm roughness has different weight for a 35 nm thick and for a 5 nm thick layer as for the 5 nm thick layer, the resulting roughness is around 1/3 of the total thickness. The observed roughness value is stable and seems to be independent from the target thickness, the material composition and the hardware parameters used. However, when considering spray coating of a material with an organic highly symmetric molecule, which would tend to crystalize, the resulting roughness and its very low dependance from the process parameters can be easily understood. The formation of the optical roughness is driven by the highly symmetric molecular structure of the BCB leading to extremely strong intermolecular interactions, therefore it is independent from the process parameters. Furthermore, it can be assumed that such high molecular symmetry could also significantly influence the layer formation. It can be assumed that the presence of small surface defects on the substrate can possibly lead to the appearance of thickness non-uniformities. An additional parameter which could lead to layer inhomogeneities for spray coating of materials with highly symmetric molecules can be the variation in the environmental conditions due to changes in the air or gas pressure, the temperature. When considering the BCB molecular structure, it can be assumed that changing the chemical structure, which would result in a symmetry breaking, could significantly decrease the measured roughness.

The AFM images for all spray coated samples show a surface roughness which confirms the findings from the VASE measurements. Interestingly, besides the total value, also the roughness morphology differs between the samples with 200 nm target layer thickness and the other samples. In the case of the 200 nm thick layer, the roughness consists of sub-nanometer particles and shows some existing sub-micrometer surface variation also. On the other hand, layers with 5 nm and 17 nm show only sub-nanometer roughness. This sub-nanometer roughness can be seen on the AFM images as small particles (size lower than 10 nm) covering the whole measured area (see Fig. 1). Below this, the sub-micrometer roughness is evident, which describes the thickness non-uniformity within the whole measured area (in the micrometer scale). In contrast to the sub-nanometer roughness, the sub-micrometer roughness is related to the layer formation and strongly influenced by the process parameters (hardware and dilution), thus different for each set up.

The presence of sub-nanometer and sub-micrometer roughness in the AFM images could explain the slightly higher measured values obtained from the VASE metrology. As ellipsometry provides only an averaged value over the measured area, such differentiation between different types of surface morphologies cannot be done and as a result, a product of both types of roughness is obtained. As already mentioned, one possible explanation of the appearing surface non-uniformity is the molecule symmetry. BCB has a highly symmetric molecule consisting of aromatic planar benzene rings and cyclic butene. In such a case it can be expected that the interaction between out of plane π- and orbitals between neighboring molecules will bring the tendency to molecular stacking. Such an effect was shown for various organic molecules with aromatic chemical groups [28,29,30,31]. The molecular stacking could easily explain the existing sub-nanometer roughness in all 3 samples but would not describe sub-micrometer differences.

b) Spray Coating Process Stability

As a next step, the spray coating process stability was tested. Batches of 25 wafers were prepared for each of the different ultrathin BCB layer target thicknesses (5 nm, 8 nm, 17 nm and 35 nm). The stability study of thicker films (with thicknesses above 50 nm) was already reported elsewhere [14]. Each wafer was analyzed with VASE using a 49-sampling points measurement. Average thickness values with standard deviations, determined for each wafer and as a function of the target thickness, are presented in Fig. 2. It can be observed that all four sets of wafers show remarkable stability of the process, which is a requirement for industrial applications. The process stability obtained for ultrathin layers follows the same trend as observed in thicker films [14,19]. The average values of the thickness and the related standard deviation on each wafer prove that the spray coating process can be very well controlled. Additionally, it shows that the variation window of the process parameters is relatively broad and can easily cover for changes occurring in the industrial environment. This is a remarkable result, especially considering that the spray coating process is determined by many parameters and material formulations.

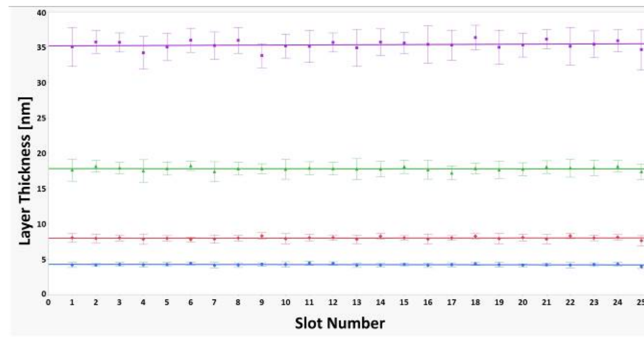

Fig.2 Mean thickness and standard deviation for different thickness layers as a function of the wafer number (batches of 25 wafers).

The long-term stability (lot-to-lot) was not studied in this work. However, as thicker films with similar wafer-to-wafer stability show also very good lot-to-lot reproducibility [14], it can be assumed that the processes studied in this work should follow the same stability path. Such assumption is reinforced by the high layer thickness homogeneity measured on the wafers.

c) Spray Coating Process Control

Finally, all process parameters were collected for all prepared layers and were compared with those used for thicker layers obtained in previous studies [14,19]. As all the measured samples showed such a good reproducibility and scalability it was considered important to understand how the process led to such a behavior. For this analysis, exemplary thicknesses were taken and compared with the material composition and spray coating process hardware parameters variations. The results are presented in Fig. 3.

Due to the high performance and control of the used spray coating equipment, the resulting spray coating thicknesses of thin and ultrathin layers with thicknesses thinner than 75 nm are mainly defined by the material dilution ratio used. As an example, layer thicknesses of 5 nm, 35 nm and 75 nm were prepared using dilutions defined as A, B and C, where A = 24 x C and B = 6 x C accordingly. For processes leading to layer thickness thinner than 75 nm, the hardware process parameters were not adjusted. In this thickness range, only the material composition was changed. To obtain thicknesses above 75 nm, only alignment of the hardware process parameters was done. In this case, mainly the nozzle speed and the dispense rate were adjusted.

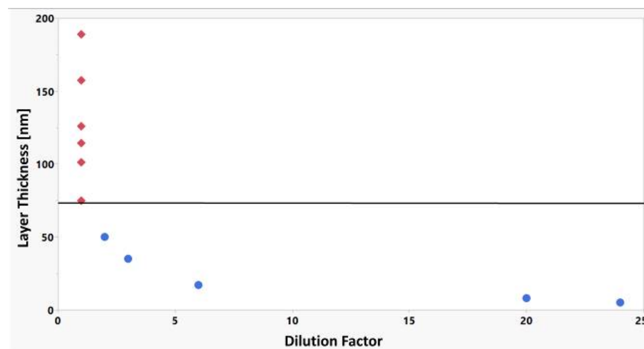

Fig.3 Layer thickness as a function of the material dilution; Thicknesses from 75 nm up are marked with red squares (dilution C) while thicknesses below 75 nm are marked with blue dots (different dilutions).

As shown in Fig. 3, the spray coating process was divided into 2 regimes where: (i) the hardware parameters play a major role (marked with red squares), and (ii) the material composition is changed by dilution as the main trigger for the layer thickness (marked with blue dots). The presence of the 2 regimes could explain the differences in the surface morphology measured by AFM and shown in Fig. 1. The sub-nanometer roughness is clearly related to the material composition and thus appears in all samples. On the other hand, the hardware adjustment is most likely causing the formation of sub-micrometer roughness as this is the only difference between the samples.

B. Ultrathin Layer Applications

a) Die-to-Wafer Bonding

A standard permanent die-to-wafer bonding process was employed to prove the industrial applicability of thin and ultrathin BCB layers. Three wafers were coated with 200 nm, 35 nm and 5 nm thick BCB layers. In the next step, pre-cut 7 x 9 mm² Si/SiO_2 dies were bonded. Multiple adhesive bonds were performed and analyzed using C-SAM metrology. Exemplary bonding results for each studied BCB layer thickness are presented in Fig. 4.

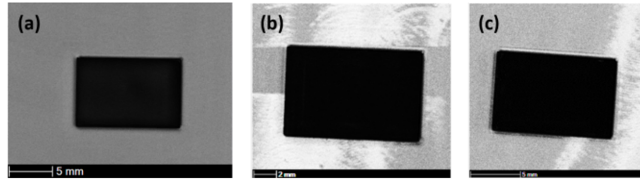

Fig.4 C-SAM images obtained for 7 x 9 mm² Si/SiO_2 dies bonded onto (a) 200 nm, (b) 35 nm and (c) 5 nm interfacial BCB layer thicknesses (black color indicates bonded area).

As can be observed, Si/SiO_2 dies were successfully bonded for each layer thickness. As the application of 200 nm layers was already proven and was used here as a reference, the use of layers with thickness below 50 nm is a significant step forward in heterogenous integration applications [5]. Besides the already mentioned lower process costs, the layer thickness downscaling should significantly improve the die alignment process as well. The advantages of ultrathin layer formation together with the remarkable thermal and mechanical properties of the BCB material, decrease post-bond misalignment budget usually caused by material shrinkage and/or reflow. On the other hand, it is important to mention that such layers demand a highly accurate defect control. In this case, spray coating seems to provide a sufficient control of the material and layer deposition process which together with the rather large process window can provide a very high process yield.

b) Micro Transfer Printing (µTP)

In industrial applications, electronic integrated circuits (EICs) as well as quantum dot laser (QDL) devices are heterogeneously integrated to Si substrates spray coated with ultrathin layers of BCB by µTP process. In the transfer printing process, one or more different sized coupons are picked up from a source wafer using polydimethylsiloxane (PDMS) stamps suitable for the coupons. The coupons are then printed on the target wafer using the BCB as adhesive bonding layer [24].

In order to study the suitability of the µTP process for ultrathin layers, at first, 25 EIC coupons with a size of 230 x 330 µm² and thickness of about 15 µm each were printed on 200 nm thick BCB deposited on Si/SiO_2 wafers as a reference. Then 5 coupons were transferred onto both 35 nm and 5 nm thick BCB layers, respectively. For all layer thicknesses the printing process resulted in 100 % yield of the EICs coupons. Fig. 5 shows exemplary microscope pictures of the coupons printed on 5 nm and 35 nm.

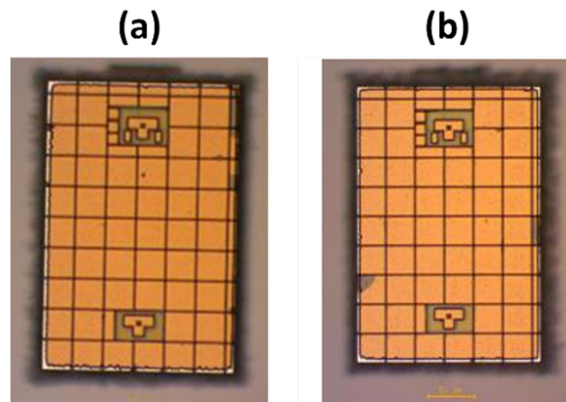

Fig. 5 EICs were micro transfer printed onto Si wafer spray coated with (a) 5 nm thick and (b) 35 nm thick BCB layers.

Additionally, a total number of 10 QDL coupons with 65 µm width and various lengths up to 2400 µm were successfully transfer printed for each BCB layer thickness. Fig. 6 illustrates the transferred coupons on the Si/SiO_2 target wafers with 5 nm and 35 nm BCB thickness.

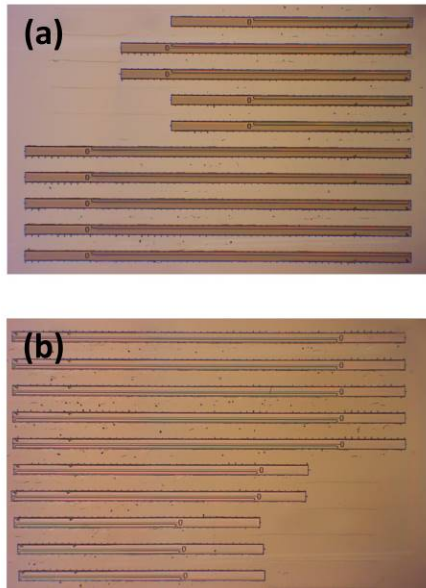

Fig. 6 Microscope images of QD laser coupons on (a) 5 nm BCB and (b) 35 nm BCB on Si substrate. Coupons are 1.5 mm, 1.8 mm and 2.4 mm long.

The total number of transfer-printed coupons for each length is given in Table 3. It can be observed that all coupons were successfully transferred, resulting in a remarkable print yield of 100 %.

TABLE III. SUMMARY OF COUPONS TRANSFER PRINTED ON SI WITH 5 NM AND 35 NM BCB.

Target	QDL amount	QDL Dimensions	Print Yield
5 nm BCB	3	1.5 mm	100 %
	2	1.8 mm	
	5	2.4 mm	
35 nm BCB	3	1.5 mm	100 %
	2	1.8 mm	
	5	2.4 mm	

IV. CONCLUSIONS

In this work, an advanced spray coating process was developed for ultrathin layer deposition. Layer thicknesses down to 5 nm were achieved, which is a huge step forward in the ultrathin layer deposition technologies. Narrow thickness value distributions show that the developed process is very stable with very good homogeneity within the wafers as well as wafer-to-wafer. Additionally, a rather large process window for the resist target layer thickness was shown, allowing for a broad industrial applicability. All layers were analyzed using variable angle spectroscopy ellipsometry which allows fast and non-destructive measurement. The homogeneity of the prepared layers was found to be well matching for a wide area of industrial applications. At first, the general applicability of ultrathin spray coated layers was tested using standard die-to-wafer bonding technology. The Si dies used for this work can substitute most advanced devices in real applications. In a second step, real devices were used. SiGe BiCMOS EICs and GaAs QD laser coupons up to 2.4 mm length were successfully integrated using the µTP process onto Si substrates with ultrathin BCB layers of 5 nm and 35 nm. A printing yield of 100 % was achieved for all printed devices. The use of ultrathin adhesives allows for a broad range of new configurations of integrated devices, with improved thermal sink. This work sets another step forward towards the efficient assembly of co-packaged optics for datacom and quantum computing applications.

ACKNOWLEDGMENT

The authors would like to thank Dr. Viorel Dragoi for his support and comments during the preparation of the manuscript.

REFERENCES

[1] M. Eibelhuber, "Enabling silicon photonics through advances in III-V integration on silicon," Semiconductor Today, 2014, 9, pp.64-67

[2] P. Kaur, A. Boes, G. Ren, T. G. Ngyuyen, G. Roelkens, A. Mitchell, "Hybrid and heterogeneous photonic integration," APL Photon, 2021, 6.

[3] F. Niklaus, P. Enoksson, E. Kälvesten, G. Stemme, "Low-temperature full wafer adhesive bonding," J. Micromech. Microeng., 2001,11.

[4] https://ase.aseglobal.com/heterogeneous-integration/ (accessed on December 11th, 2023)

[5] M. Grucela-Zajac, M. Filapek, L. Skorka, J. Gasiorowski, E. D. Glowacki, H. Neugebauer, E. Schab-Balcerzak, “Thermal, optical, electrochemical, and electrochromic characteristics of novel polyimides bearing the Acridine Yellow moiety,” Mater. Chem. Phys., 2012, 137, 221.

[6] J.E. Mark, “Physical Properties of Polymers Handbook,” Springer New York, NY 2006.

[7] P. Meredith, C. Bettinger, M. Irimia-Vladu, A. Mostert, P. Schwenn, “Electronic and optoelectronic materials and devices inspired by nature,” Rep. Prog. Phys., 2013, 76.

[8] S. Stankovic, R. Jones, M. Sysak, J. Heck, G. Roelkens, D. Thourhout, “Hybrid III-V/Si Distributed-Feedback Laser Based on Adhesive Bonding,”IEEE Photonics Technology Letters., 2012 24.

[9] A. Extance, “Adhesives & Sealants Industry,” 2009, Troy Vol. 16, Iss. 2, p.26-28

[10] N. Kim, H. Choe, M. Shah, D. Lee, S. Hur, “High-Density Patterned Array Bonding through Void-Free Divinyl Siloxane Bis-Benzocyclobutene Bonding Process,” Polymers, 2021

[11] S. Stankovic, R. Jones, J. Heck, M. Sysak, D. Thourhout, G. Roelkens, “Hybrid III-V/Si Distributed-Feedback Laser Based on Adhesive Bonding,” Electrochemical and Solid-State Letters, 2012 14.

[12] F. Niklaus, G. Stemme, J.-Q. Lu, R.J. Gutmann, “Adhesive Wafer Bonding,” Journal of Applied Physics, 2006, 99, 031101.

[13] S. Keyvaninia, M. Muneeb, S. Stankovic, G. Roelkens, D. Thourhout, J. Fedeli, “A highly efficient electrically pumped optical amplifier integrated on a SOI waveguide circuit,” presented at 16th European Conference on Integrated Optics, Barcelona, Spain, 2012.

[14] J. Rimböck, J. Gasiorowski, M. Pires, T. Zenger, J. Burggraf, V. Dragoi, “Adhesive Wafer Bonding Using Ultra-Thin Spray-Coated BCB Layers,” ECS Trans., 2020

[15] R. Loi, J. O'Callaghan, B. Roycroft, Z. Quan, K. Thomas, A. Gocalinska, E. Pelucchi, A.J. Trindade, C. A. Bower, B. Corbett, “Thermal Analysis of InP Lasers Transfer Printed to Silicon Photonics Substrates,” J. Lightwave Technol., 2018, 36, 5935-5941.

[16] S. Keyvaninia, M. Muneeb, S. Stankovic, P.J. Veldhoven, D. Thourhout, G. Roelkens, “Ultra-thin DVS-BCB adhesive bonding of III-V wafers, dies and multiple dies to a patterned silicon-on-insulator substrate,” Optical Materials Express., 2013, 3.10.136.

[17] F. Niklaus, R. Kumar, J. McMahon, J. Yu, T. Matthias, M. Wimplinger, P. Lindner, J.Q. Lu, T.S. Cale, R.J. Gutmann, “Effects of Bonding Process Parameters on Wafer-to-Wafer Alignment Accuracy in Benzocyclobutene (BCB) Dielectric Wafer Bonding,” in Mater. Res. Soc. Symp. Proc., January 2005.

[18] C. Brubaker, M. Wimplinger, P. Lindner, S. Pargfrieder, “Investigating the use of spray-coating technology in MEMS applications,” presented at MICRO, Santa Monica, March 2004, 22, 45-55.